Optics Communications 282 (2009) 4119–4123

Contents lists available at ScienceDirect

Optics Communications

journal homepage: www.elsevier.com/locate/optcom

Photoetching of spherical microlenses on glasses using a femtosecond laser

Hewei Liu [a], Feng Chen [a,*], Xianhua Wang [a], Qing Yang [b], Dongshi Zhang [a], Jinhai Si [a], Xun Hou [a]

[a] Key Laboratory for Physical Electronics and Devices of the Ministry of Education and Shaanxi Key Laboratory of Photonic Technology for Information, School of Electronics and Information Engineering, Xi'an Jiaotong University, No. 28, Xianning West Road, Xi'an 710049, PR China
[b] State Key Laboratory for Manufacturing Systems Engineering, Xi'an Jiaotong University, No. 28, Xianning West Road, Xi'an 710049, PR China

ARTICLE INFO

Article history:
Received 28 April 2009
Received in revised form 8 July 2009
Accepted 8 July 2009

PACS:
42.62.−b
42.79.Bh
81.05.K

Keywords:
Microlenses
Femtosecond laser pulses
Laser direct writing
Glasses

ABSTRACT

We fabricated spherical microlenses on optical glasses by femtosecond laser direct writing (FLDW) in ambient air. To achieve good appearances of the microlenses, a meridian-arcs scanning method was used after a selective multilayer removal process with spiral scanning paths. A positive spherical microlens with diameter of 48 μm and height of 13.2 μm was fabricated on the surface of the glass substrate. The optical performances of the microlens were also tested. Compared to the conventional laser direct writing (LDW) technique, this work could provide an effective method for precise shape-controlled fabrication of three-dimensional (3D) microstructures with curved surfaces on difficult-to-cut materials for practical applications.

1. Introduction

Microlenses and microlens arrays are extensively used in a wide range of applications, such as collimation of lasers, optical computing and photonic imaging [1–3]. Present techniques for the fabrication of microlenses, which mainly include photo-resist reflow technique [4], moving pattern lithography technique [5], gray-tone photolithography technique [6], are difficult to meet the demands of high precision and simple process. In the past decades, a significant amount of works has been carried on laser direct writing (LDW) techniques. For example, a F_2 laser was adopted to ablate and form microlenses on the end faces of hard-clad silica fibers by a rotational scanning technique. However, a mismatch of the fiber rotation axis resulted in some surface irregularities of the fabricated microlenses and the laser-ejected melt could be observed due to the thermal effects [7]. Moreover, contour scanning techniques were introduced to fabricate spherical microlenses on optical polymers using an ArF laser [8]. Guo et al. reported the fabrication of microlenses with arbitrary shape by femtosecond laser two-photo photopolymerization (TPP) technique [9]. However, these techniques can only be used for the processing of photopolymers. It still remains difficulties for precise fabrication of high-aspect-ratio microstructures, in particular with curved surfaces, on glasses which combine chemical inertness with better mechanical, thermal and optical properties than photopolymers.

Femtosecond laser ablation process provides an effective method for the fabrication of three-dimensional (3D) microstructures on a series of difficult-to-cut materials, such as glasses [10], metals [11], and ceramics [12]. The micro-regions of these materials, when irradiated by focused femtosecond laser pulses with the energies higher than material ablation thresholds, would be etched out and 3D microstructures could be fabricated in this top-down processing way. Over the past decades, femtosecond laser-assisted wet etching technique was widely applied in micromachining of 3D structures [13,14]. In recent years, a multi-step processing method, which combines procedures of femtosecond laser direct writing, thermal treatment, chemical wet etching and postannealing, was employed to fabricate 3D optical components, such as micro-mirrors [15], microlenses [16] and an integration of micro-mirrors and microlenses [17]. This technique is suitable for fabrication of complex 3D structures embedded in photosensitive glasses. Here we use a femtosecond laser dry etching technique based on LDW for precise fabrication of spherical microstructures. The technique could be used for precise processing of a wide range of materials. It is essential to optimize the ablation parameters to accurately control the removal volume of materials by each pulse. Furthermore, the obstruction of debris and residual thermal effects should also be avoided in order to obtain smooth surfaces.

* Corresponding author. Tel./fax: +86 29 82663485.
E-mail address: chenfeng@mail.xjtu.edu.cn (F. Chen).

0030-4018/$ - see front matter © 2009 Elsevier B.V. All rights reserved.
doi:10.1016/j.optcom.2009.07.017

In this paper, we present a precise micromachining process that is based on femtosecond laser ablation for the fabrication of 3D microstructures with curved surface, which has great potential applications in Micro Electromechanical System (MEMS), micro optics devices, and medical micro devices, etc. As an example, positive spherical microlenses were fabricated on the surface of glasses in ambient air. In the processing procedures, we at first employed a selective multilayer removal process with spiral scanning paths to get a tough spherical cap structure, and subsequently utilized a meridian-arcs smooth process to achieve a good appearance of the microlens. The experimental results indicate that the thermoelastic shock wave plays an important role during the process of femtosecond laser ablation of glasses in ambient air when pulse energies are well above the ablation thresholds. The dependence of processing quality on ablation parameters was also discussed.

2. Fabrication process

For the experiments, the sample was a 15 × 15 mm^2 K9 optical glass substrate with the thickness of 3 mm. The laser source was a Ti: sapphire oscillator–amplifier system (FEMTOPOWER Compact Pro, FEMTOLASERS), which delivered 800 nm, 30 fs Gaussian laser pulses at a repetition rate of 1 kHz. A 50× microscope objective (Olympus, NA = 0.5) focused the laser beam onto the sample surface. The incident pulse energy could be continuously varied by a variable attenuator and a mechanical shutter was employed to control the transit of laser beam. The sample was fixed onto a computer-controlled three-axis stage (M-505.2DG, Physik Instrumente), following a preprogrammed pattern. The machining process was monitored by a CCD camera.

In the initiation of the processing procedures, the microlens was fabricated by a selective multilayer removal process. As depicted in Fig. 1a, a sequential accumulation of annular-shape regions was removed layer-by-layer in a top-down method. For each layer, the sample was continuously translated in a spiral pattern and the laser pulses removed the materials of the annular-shape region by such spiral scanning path with a constant tangent velocity. In this experiment, the interval of the spiral, λ, was set to 1 μm, which is smaller than the diameter of the focal spot. The outer radius, Φ_o, of the annular-shape regions is represented by $\Phi_o = R + \lambda$, where R is the designed radius of the microlens, and was fixed to 25 μm in the experiment. The inner radiuses Φ_i of each layer can be determined by:

$$\Phi_1 = \left[R^2 - (R - l_1)^2\right]^{\frac{1}{2}}$$

$$\Phi_i = \left[R^2 - \left(R - \sum_{j=1}^{i-1} l_j\right)^2\right]^{\frac{1}{2}} \quad (i \geqslant 2)$$

Here, i is the layer ordinal and l_j is the thickness or step size of the layer j in vertical directions. After the removal process was finished in one layer, the sample was returned to the starting point and then stepped towards the objective for the distance l_j, followed by the removal process of the next layer. Other parameters of the microlenses are: $R = 24$ μm, $l_j = 2.5$ μm and the height of the spherical cap $H = 15$ μm.

The multilayer process has been widely used for the micromachining of 3D microstructures by the TPP technique [9,18]. The precision of the fabricated 3D microstructures are sensitive to layer thickness. A smaller layer thickness is essential for a better appearance, but necessitates a large number of processing layers and longer processing time. Moreover, it is not suitable to obtain curved surfaces with good appearance only by means of multilayer removal process. Therefore, after the multilayer removal process, air flow was used to clean the debris deposited on the spherical cap and subsequently, a special smooth process was provided to minimize the processing layers and improve processing quality, as shown in Fig. 1b. The focal point scanned the surface along a meridian-arc path of the spherical cap fabricated by the multilayer process. Subsequently, the sample rotated clockwise by the center axis of the spherical cap for 1° and then the focal point scanned along another meridian arc path. This process repeated until the surface of the spherical cap was totally scanned by femtosecond laser pulses. In our experiments, the smooth process was totally consisted of 360 meridian-arcs, which guaranteed the intervals between adjacent arcs smaller than ablation width. After photoetched, the sample was immersed and treated in ultrasonic bath for 5 min both in water and acetone in order to clean the residual ejections of material off the curve surface.

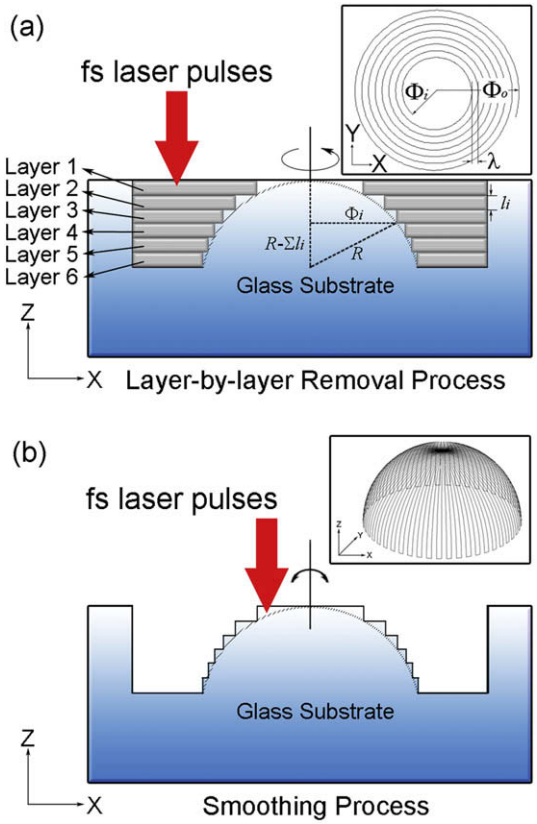

Fig. 1. Schematic of the fabrication procedures of spherical microlens: (a) the layer-by-layer removal process. Shadow regions show the regions would be removed by the laser pulses. Materials were eliminated from Layer 1 to Layer 6 by spiral scanning path. (b) The smooth process by a meridian-arcs scanning path.

3. Results and discussion

3.1. Optimization of parameters

In the past, micromachining of materials was carried out in different processing environments. The most common one was water-assisted process [19,20]. It is believed that the presence of water enhances the machining quality by removing the ablation debris and cooling the material efficiently. Unfortunately, for the precise microfabrication, bubbles generated by vaporization and ionization of water should be minimized to avoid disturbances. Therefore, the pulse energy was limited close to the threshold fluence of the optical breakdown and processing velocity was also relatively low, which would reduce the processing efficiency. Moreover, processing of some hard-to-cut materials with high

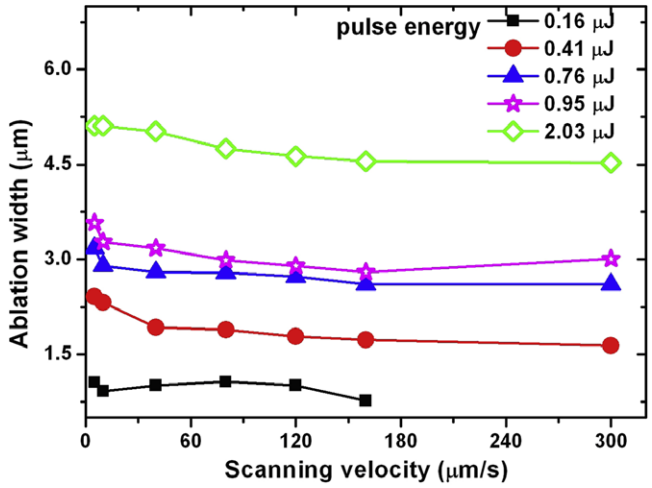

Fig. 2. Dependence of ablation width of the micro-lines on the scanning velocities and pulse energies. The scanning velocities ranged from 5 to 300 μm/s and the pulse energies were 0.16, 0.41, 0.76, 0.95, and 2.03 μJ, respectively.

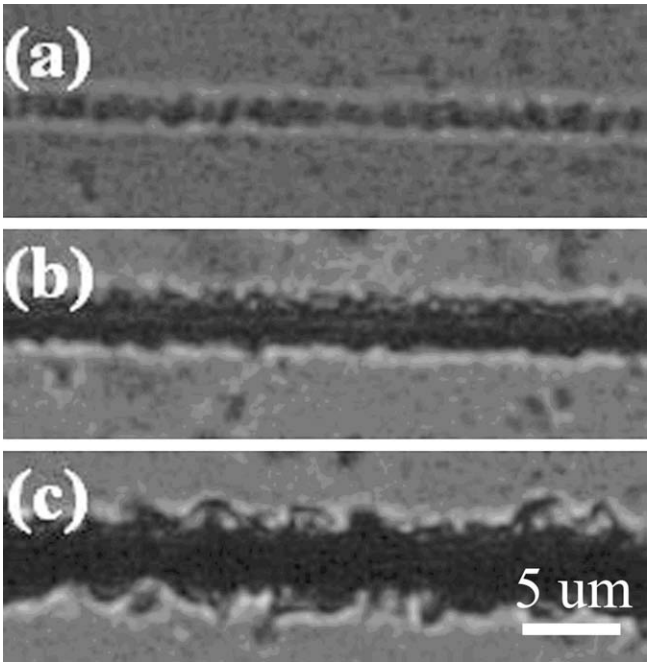

Fig. 3. Optical images of the ablated micro-lines. The scanning velocity was kept at 80 μm/s. The pulse energy was set at (a) 0.16 μJ, (b) 0.41 μJ, (c) 0.76 μJ, respectively. We can see that ablation width increased sharply with the increase of pulse energy. When the pulse energy enhanced to 0.76 μJ, cracks can be observed.

ablation threshold requires high-power incident laser beams, and the intense disturbances of water are inevitable. In our experiments, microlenses were fabricated in ambient air. Material volume removed per pulse could be maximized with the pulse energy well above the ablation threshold and scanning velocity would be increased too. The influence of ablation parameters on processing quality was necessary for optimization of parameters.

In order to optimize the ablation parameters in such high efficiency process, we investigated the influence of the processing quality on pulse energies and scanning velocities. By varying the power of the incident laser beam and scanning velocity, a series

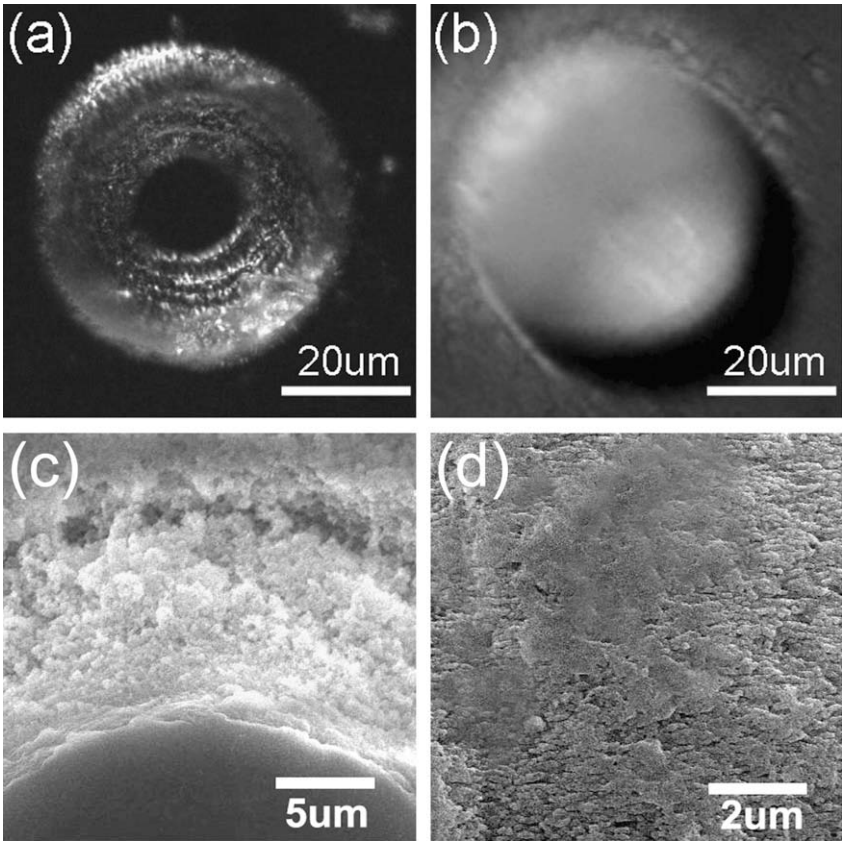

Fig. 4. Optical microscope images of the microlenses fabricated without (a) and with (b) the smooth process. SEM images of the surface morphologies before and after the smooth process are presented in (c) and (d), respectively.

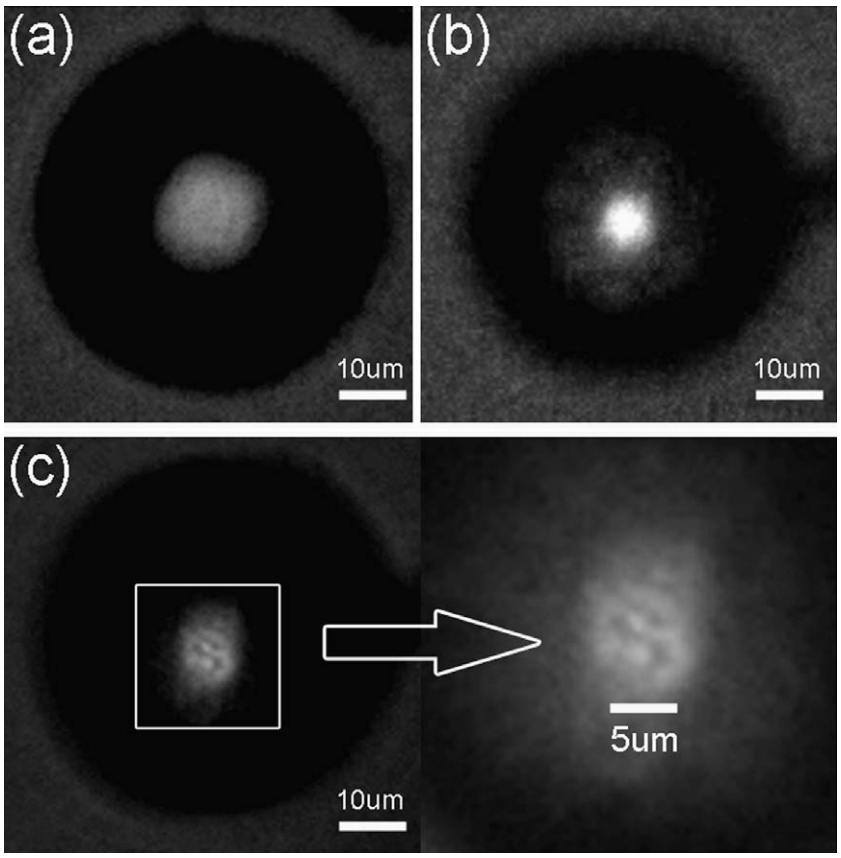

Fig. 5. Optical performances of the microlenses: (a) The focusing properties of the microlenses shown in Fig. 4a. (b) The focusing properties of the microlens shown in Fig. 4b. A focal spot with diameter of around 5 μm was obtained near the optical axis. (c) Imaging ability of the spherical microlens with the smoothing process.

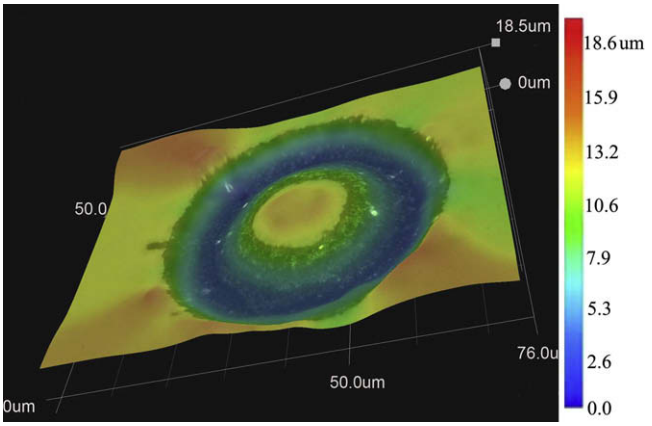

Fig. 6. 3D profile of the fabricated microlens with the smooth process. Some uplifts with height of 1–2 μm were observed around the processing region.

of straight micro-lines was ablated on the surface of the sample in ambient air, and then the widths of these lines were measured via an optical microscope. Fig. 2 shows the dependence of ablation widths on pulse energies and scanning velocities. We can see that the widths of ablated lines are slightly decreased with the increase of scanning velocity at such energy level. However, the ablation widths increased sharply with the increase of the pulse energy. From the Fig. 2, we can also observe that the ablation widths were much larger than the diameter of the focal point when the pulse energies were higher than 0.41 μJ. In the case of intense femtosecond laser ablation of solids, Coulomb explosion [21] and the thermoelastic shock wave [22] were proposed to explain the femtosecond laser ablation of materials. After the sample was irradiated by femtosecond laser pulses, Coulomb explosion caused by the localized charge imbalance took place at first. Following, pulse-energy-resolved thermoelastic shock wave formed, the inwards of which produced fragmentation of surrounding materials and leaded to a more removal volume than the irradiated region, and the outwards released of repelling force to push the ablation debris away from the irradiated regions. When the pulse energy was several times above the ablation threshold, the thermoelastic shock wave was extremely strong, and dominated the dynamic process of femtosecond laser ablation. Accordingly, the ablation width was sensitive to the pulse energy rather than scanning velocity.

In addition, we have observed the volumes of ablation debris and fringe appearances of the ablated lines. In general, when the lines ablated in lower pulse energies, less ablated ejections were produced and better fringe appearances were obtained. However, in the process of fabrication of microlenses, when pulse energy was lower than 0.3 μJ, thermoelastic shock wave was not strong enough to push ejections far away and deposition of the ablation debris scattered the incident laser, hindering the subsequent process. With the increased of pulse energy, thermoelastic shock wave became strong and could help cleaning the processing areas. Whereas, when the pulse energy increased to 0.76 μJ, the fabricated micro-line has a poor fringe appearance, as shown in Fig. 3c. Moreover, lower scanning velocities need a longer processing time, but achieve a better processing quality than fast processes. Considering both the processing efficiency and quality, different parameters were employed in the multilayer removal process and the smooth process. In the multilayer removal process, the pulse energy and scanning velocity were 0.4 μJ and 160 μm/s.

The layer thickness l_j = 2.5 μm, which is close to the ablation depth when pulse energy is 0.4 μJ. In the smoothing process, accurate and gentle ablation was essential to obtain a good surface appearance. The pulse energy was reduced to 0.2 μJ and scanning velocity was 80 μm/s. The whole processing time for fabricating a microlens with a diameter around 50 μm was about 15–20 min.

Optical microscope images of the fabricated microlenses without and with the smooth process are shown in Fig. 4a and b, respectively. Scanning electron microscope (SEM) images of the surfaces before and after the smooth process are also presented in Figs. 4c and 3d. The processing parameters are aforementioned. From the figures, we can observe that the microlens fabricated only by the multilayer process has a flat top (Fig. 4a), which is the residual materials not etched by the spiral scanning paths. The flat top was removed by the following smooth process and a positive spherical microlens was fabricated, as shown in Fig. 4b. The SEM images of the surface morphologies apparently indicate that the surface obtained only by the multilayer process is rough (Fig. 4c), which has a roughness of about 2–3 μm. After the smooth process, it became smoother (Fig. 4d) and surface roughness is reduced to less than 200 nm. Therefore, the smooth process enables us to fabricate microlenses with smoothness surfaces.

3.2. Optical performances tests

To demonstrate optical performances of the two microlenses fabricated with and without the smooth process, we measured their focusing properties using an optical microscope. The optical arrangement can be found in reference [9]. The focal length was measured to be about 120 μm. The results are shown in Fig. 5. The surface of the microlens shown in Fig. 4a is scabrous, so the focusing spot is not as good as the microlens fabricated with the smooth process. Imaging ability of the micro spherical lens was also tested by a system equipped with a microscope. A sheet of paper with a printed letter "S" which was about 1 mm wide and 1.5 mm high was set between fabricated microlens and light source, and the image of the letter was captured between the microlens and objective, as shown in Fig. 5c. From the Fig. 5c, a hazy zone could be observed surrounding the image. The hazy zone might be attributed to the residual surface roughness after the smooth process, as shown in Fig. 4d. This surface roughness is in nanometer scales and can be commonly seen on almost all kinds of solids after irradiated by femtosecond laser pulses. In addition, microlens without the smooth process failed to obtain any images due to its micrometer-sized roughness and the flat top.

3.3. Dimensional measurements

Subsequently, a Color 3D Laser Scanning Microscope (VK-9700, KEYNECE) was used for dimensional measurements and morphological characterizations. Fig. 6 shows the 3D profile of the fabricated microlens. The measuring results indicate that the diameter of the microlens is 48 μm, and the height is 13.2 μm. Compared to the microlenses fabricated by F_2 and ArF laser, femtosecond laser could be used for precise fabrication of microlenses in smaller sizes [7,8]. Note that both positive and negative spherical microlenses with different sizes can be fabricated by our technique, and smaller microlenses can be achieved using microscope objectives with larger numerical aperture (NA).

4. Conclusions

In summary, a multilayer removal process combined with a special smooth process based on femtosecond laser ablation was introduced to fabricate spherical microlenses on the surface of optical glasses in ambient air. After the optimization of some important processing parameters, a spherical positive microlens with the diameter of around 48 μm was obtained. The experimental results showed that the thermoelastic shock wave can increase the ablation rate and shockwave will help for cleaning the ablation debris. The optical performances of the fabricated microlenses indicate that this technique is suitable for the fabrication of truly 3D micro-optical devices and structures with accurately controllable-shape on various difficult-to-cut materials.

Acknowledgement

The authors gratefully acknowledge the financial support for this work provided by the National Science Foundation of China under the Grant Nos. 60678011 and 10674107.

References

[1] B. Messerschmidt, T. Possmer, R. Gohring, Appl. Opt. 34 (1995) 7825.
[2] K. Hamanaka, H. Nemoto, M. Oikawa, E. Okuda, T. Kishimoto, Appl. Opt. 29 (1990) 4064.
[3] K.H. Jeong, G. Liu, N. Chronis, L. Lee, Opt. Express 12 (2004) 2494.
[4] P. Nussbaum, R. Völkel, H.P. Herzig, M. Eisner, S. Haselbeck, Pure Appl. Opt.: J. Euro. Opt. Soc. Part A 6 (1997) 617.
[5] S. Sugiyama, S. Khumpuang, G. Kawaguchi, J. Micromech. Microeng. 14 (2004) 1399.
[6] J. Yao, Z. Cui, F. Gao, Y. Guo, C. Du, H. Zeng, C. Qiu, Microelectron. Eng. 57–58 (2001) 729.
[7] T. Fricke-Begemann, J. Li, J. Ihlemann, P.R. Herman, G. Marowsky, Int. Soc. Opt. Eng. 5578 (1) (2004) 589.
[8] Y.T. Chen, K. Nawssens, R. Baets, Y.S. Liao, A.A. Tseng, Opt. Rev. 12 (2005) 427.
[9] R. Guo, S.Z. Xiao, X.M. Zhai, J.W. Li, A.D. Xia, W.H. Huang, Opt. Express 14 (2006) 810.
[10] A.B. Yakar, R.L. Byer, J. Appl. Phys. 96 (2004) 5316.
[11] E.G. Gamaly, A.V. Rode, B.L. Davies, V.T. Tikhonchuk, Phys. Plasmas 9 (2002) 949.
[12] N. Bärsch, K. Werelius, S. Barcikowski, F. Liebana, U. Stute, A. Ostendorf, J. Laser Appl. 19 (2007) 107.
[13] M. Masuda, K. Sugioka, Y. Cheng, T. Hongo, K. Shihoyama, H. Takai, I. Miyamoto, K. Midorikawa, Appl. Phys. A 78 (2004) 1029.
[14] Matsuo, S. Kiyama, Y. Shichijo, T. Tomita, S. Hashimoto, Y. Hosokawa, H. Masuhara, Appl. Phys. Lett. 93 (2008) 051107.
[15] Y. Cheng, K. Sugioka, K. Midorikawa, M. Masuda, K. Toyoda, M. Kawachi, K. Shihoyama, Opt. Lett. 28 (2003) 1144.
[16] Y. Cheng, H.L. Tsai, K. Sugioka, K. Midorikawa, Appl. Phys. A 85 (2006) 11.
[17] Z. Wang, K. Sugioka, K. Midorikawa, Appl. Phys. A 89 (2007) 951.
[18] S. Park, S. Lee, D. Yang, H. Kong, K. Lee, Appl. Phys. Lett. 87 (2005) 154108.
[19] C. Li, X. Shi, J. Si, T. Chen, F. Chen, A. Li, X. Hou, Opt. Commun. 282 (2009) 657.
[20] R. An, M.D. Hoffman, M.A. Donoghue, A.J. Hunt, S.C. Jacobson, Opt. Express 16 (2008) 15206.
[21] W.G. Roeterdink et al., Appl. Phys. Lett. 82 (2003) 4190.
[22] X. Wang, X. Xu, J. Therm. Stresses 25 (2002) 457.